Analyst

PAPER

View Article Online
View Journal

Published on 26 March 2025. Downloaded by Shanghai Normal University on 3/28/2025 7:46:19 AM.

Check for updates

Cite this: DOI: 10.1039/d5an00189g

A DNA concatemer-encoded CRISPR/Cas12a fluorescence sensor for sensitive detection of Pb^{2+} based on DNAzymes†

Shaoying He,‡[a,b] Wei Lin,‡[c] Xin Liu,[a,b] Fei Li,[c] Hong Liang,[d] Huo Xu, *[b] Chunhua Lu *[c] and Chao Xing*[a,b]

Received 20th February 2025,
Accepted 13th March 2025

DOI: 10.1039/d5an00189g

rsc.li/analyst

Lead pollution presents a significant threat to ecological systems and human health, underscoring the urgent need for highly sensitive detection methods. Herein, we introduce a novel DNA concatemer-encoded CRISPR/Cas12a fluorescence sensor (MDD-Cas12a) for sensitive detection of Pb^{2+} based on DNAzymes. To accomplish this, we designed a substrate strand containing a long DNA concatemer encoding multiple protospacer adjacent motifs (PAMs) and protospacer sequences for activation of the CRISPR/Cas12a system. The DNA concatemer was subsequently anchored to the surface of magnetic beads (MBs) to fabricate a MBs-DNA concatemer nanoprobe. In the presence of Pb^{2+}, the DNAzyme structure catalyzes the cleavage of the substrate strand, leading to the release of DNA concatemers. Following magnetic separation, the released DNA concatemers significantly activate the non-specific trans-cleavage activity of the Cas12a/crRNA complex. The fluorescence reporter DNA is then completely cleaved by the activated Cas12a/crRNA complex, and the Pb^{2+} concentration in the sample can be quantified by measuring the fluorescence signal. By harnessing the specific recognition capability of DNAzymes for Pb^{2+}, the programmability of DNA concatemers, and the self-amplification features of the CRISPR/Cas12a system, the MDD-Cas12a platform demonstrates high sensitivity and specificity for detecting Pb^{2+} in milk and lake water samples.

Introduction

The pervasive presence of heavy metals in the environment, particularly lead ions (Pb^{2+}), poses a grave threat to both ecological systems and human health.[1] The development of accurate and rapid detection technologies has become increasingly urgent. These technologies not only help in tracking and managing environmental lead contamination but also play an essential role in safeguarding public health by preventing lead exposure. Traditional methods for detecting Pb^{2+}, such as inductively coupled plasma mass spectrometry (ICP-MS),[2] atomic absorption spectrometry (AAS),[3] and atomic emission spectrometry,[4] are highly sensitive and accurate. However, these techniques come with significant drawbacks: they require expensive and complex equipment, skilled technicians, and extensive labor.[5] These factors make traditional methods less feasible for rapid, on-site testing and limit their application in real-time environmental monitoring. In response to these limitations, there has been a push to develop simpler, cost-effective, and rapid detection methods for Pb^{2+} detection.

DNAzymes are specifically engineered single-stranded DNA molecules with enzymatic capabilities for specific substrates, and are derived from systematic *in vitro* screening processes of SELEX.[6] DNAzymes exhibit many excellent properties, such as stability, ease of synthesis, low cost, and high specificity for their target ions.[7] Pb^{2+}-specific DNAzymes, such as 8–17 and GR-5, which activate and cleave specific substrate strands in the presence of Pb^{2+}, have emerged as a powerful recognition element in the construction of Pb^{2+} biosensors with different signal formats such as fluorometry, colorimetry and electrochemistry.[8] Moreover, the integration of DNAzymes with other nucleic acid signal amplification techniques enables the establishment of highly sensitive and specific sensing platforms.

Clustered regularly interspaced short palindromic repeats (CRISPR) and their associated Cas proteins (CRISPR/Cas) were

[a]College of Environment and Safety Engineering, Fuzhou University, Fuzhou 350116, P.R. China. E-mail: chaoxing@mju.edu.cn
[b]College of Materials and Chemical Engineering, Minjiang University, Fuzhou 350108, P.R. China. E-mail: chemicalxuhuo@163.com
[c]College of Chemistry, Fuzhou University, Fuzhou 350116, P.R. China. E-mail: chunhualu@fzu.edu.cn
[d]College of Geography and Oceanography, Minjiang University, Fuzhou 350108, P.R. China

†Electronic supplementary information (ESI) available. See DOI: https://doi.org/10.1039/d5an00189g

‡These authors contributed equally.

Published on 26 March 2025. Downloaded by Shanghai Normal University on 3/28/2025 7:46:19 AM.

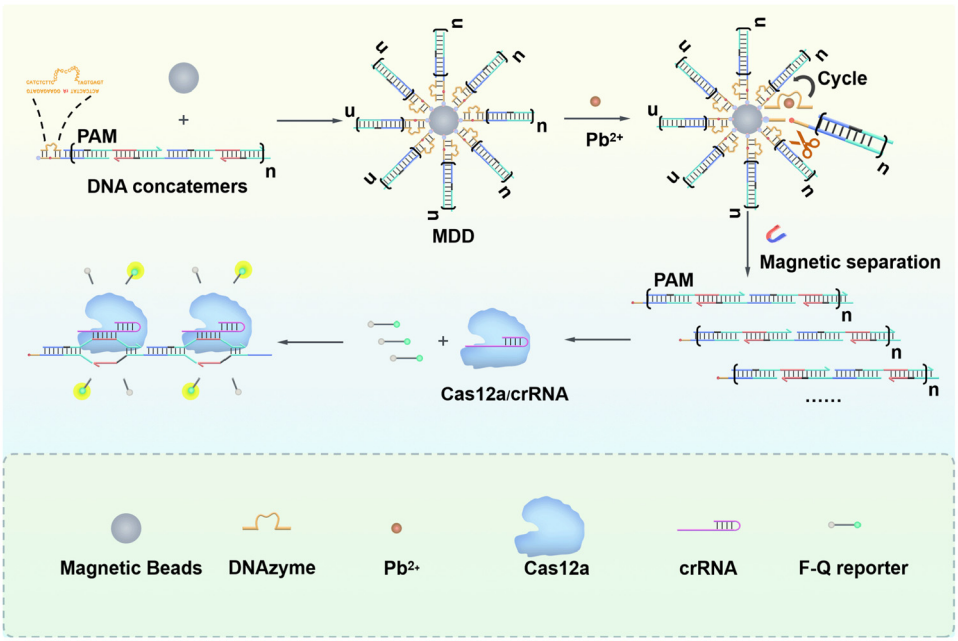
initially identified as part of the adaptive immune system in bacteria, protecting against viral infections.[9–11] Beyond its renowned gene-editing capabilities, the CRISPR/Cas system has been effectively utilized in molecular detection.[12–20] Among its diverse proteins, Cas12a is particularly notable for its distinctive trans-cleavage activity. This trans-cleavage activity allows Cas12a to cleave single-stranded DNA non-specifically after the initial target recognition, enhancing signal amplification in biosensor assays.[21–23] Numerous CRISPR/Cas12a-based sensors have been developed to sensitively detect nucleic acids, proteins, and small molecules, even in complex biological samples.[24–27] While CRISPR/Cas12a holds significant promise for biosensing applications, its effectiveness is limited by the sequence-specific nature of guide RNA targeting. This dependency mandates a pre-amplification step utilizing isothermal amplification methods such as RCA[28] and loop-mediated isothermal amplification (LAMP).[29] However, integrating these additional procedures adds complexity and time to the assay process. Hence, there is a pressing need to explore more streamlined DNA amplification strategies that can seamlessly complement CRISPR/Cas12a for the creation of biosensors tailored for detecting Pb^{2+}.

Herein, we present an innovative Pb^{2+} fluorescence sensing platform (MDD-Cas12a) that integrates magnetic beads (MBs), DNAzyme, DNA concatemers, and CRISPR/Cas12a. As depicted in Scheme 1, long DNA concatemers encoding multiple protospacer adjacent motifs (PAMs)[23,30–32] and protospacer sequences were assembled *via* substrate strand-triggered hybridization chain reactions (HCRs).[33–35] The substrate strand containing DNA concatemers was anchored to the surface of MBs through the biotin–streptavidin interaction. In the presence of Pb^{2+}, the DNAzyme structure catalyzes the cleavage of the substrate strand, leading to the release of DNA concatemers. Following magnetic separation, the released DNA concatemers significantly activate the non-specific trans-cleavage activity of the Cas12a/crRNA complex. The fluorescence reporter DNA is then completely cleaved by the activated Cas12a/crRNA complex, and the Pb^{2+} concentration in the sample can be quantified by measuring the fluorescence signal. In the absence of the target Pb^{2+}, the DNA concatemers loaded on the MBs remain intact, and the activity of CRISPR/Cas12a is not initiated, resulting in low fluorescence signals. By leveraging the specific Pb^{2+} recognition ability of DNAzymes, the programmability of DNA concatemers, and the self-amplification capability of the CRISPR/Cas12a system, the MDD-Cas12a platform exhibits high sensitivity and specificity for Pb^{2+} detection in milk and lake water samples. This platform could enrich and advance the development of new strategies for practical environmental analysis.

Materials and methods

Materials and chemical reagents

All oligonucleotide chains used in this study were purchased from Shangya Biotechnology Co., Ltd (Fuzhou, China). The detailed sequences of oligonucleotide chains are provided in Table S2.† Streptavidin-modified magnetic beads were obtained from Xianfeng Nanomaterial Technology Co., Ltd (Jiangsu, China). EnGen® LbaCas12a (Cpf1) was sourced from New England Biological Laboratories Limited (Beijing, China). Lead nitrate, magnesium chloride, and sodium chloride were procured from Aladdin (Shanghai, China). All chemical reagents were of reagent grade.



Scheme 1 Schematic illustration of the MDD-Cas12a system for Pb^{2+} detection.

 This journal is © The Royal Society of Chemistry 2025

Published on 26 March 2025. Downloaded by Shanghai Normal University on 3/28/2025 7:46:19 AM.

Buffers used in this work are as follows:

• Buffer A: 10 mM Tris–HCL, 50 mM NaCl, 10 mM $MgCl_2$, pH = 7.2,

• Buffer B: 20 mM Tris–HCL, 1 M NaCl, 0.0015% TritonX-100, pH = 7.6,

• Buffer C: 10 mM Tris–HCL, 50 mM NaCl, pH = 7.4.

Preparation of the DNA concatemers

DNA concatemers were designed through the self-assembly of hybrid chain reactions (HCRs). 10 μM stem-loop structures H1 and H2 were first annealed in Buffer A, respectively (heated in a 95 °C metal bath for 10 minutes, then naturally cooled to room temperature over 10 minutes to stabilize the stem-loop structure). In the second step, 200 nM substrate-initiating strand (ST) and 500 nM H1 and H2 were mixed in Buffer A and incubated at 37 °C for 60 minutes. The long DNA concatemers containing multiple protospacer adjacent motifs (PAM) and protospacer sequences were prepared and stored at 4 °C.

Preparation of the MBs-DNA concatemer (MDD) complexes

First, the DNA concatemers containing the biotin-substrate strand (ST) were mixed with 0.1 mg mL^{-1} streptavidin-MBs in Buffer B and incubated for 2 hours at 37 °C. Then, the dissociative DNA concatemers were removed by magnetic separation, and the MBs-DC was purified with ultrapure water 6–8 times.

Detection of Pb^{2+} by MDD-Cas12a

First, MBs-DC, DNAzymes, and various concentrations of Pb^{2+} were mixed in Buffer C and incubated at 37 °C for 60 minutes. Subsequently, the released DNA concatemers were purified by magnetic separation. Meanwhile, Cas12a (100 nM) was mixed with crRNA (50 nM) in 1× NEBuffer 2.1 and incubated at 37 °C for 30 minutes to form the Cas12a/crRNA complexes. Then, 2 μL of DNA concatemers and 1 μL of reporter (20 μM) were added to the preassembled Cas12a/crRNA complexes to a final volume of 20 μL, and incubated at 37 °C for 60 minutes. The successive fluorescence changes were monitored at a fixed emission wavelength of 520 nm with fixed excitation at 490 nm.

Results and discussion

The construction of the MDD-Cas12a system

To construct the MDD-Cas12a detection system, DNA concatemers containing PAM and protospacer sequences were synthesized using the hybridization chain reaction (HCR, Fig. 1A). The substrate-trigger sequences (ST), which contain the substrate strand (SS, yellow part) and the trigger strand (TS, blue part), were rationally designed to trigger the HCR. Native polyacrylamide gel electrophoresis (PAGE) was first conducted to confirm the successful construction of the DNA concatemers. As shown in Fig. 1B, H1 and H2 remained stable individually (lanes 2–3), and no hybridization product was observed when only H1 and H2 were mixed (lane 4). The typical HCR product with low mobility was observed only after incubation of H1, H2, and ST (lane 6), indicating the assembly of DNA concatemers with the addition of ST. Furthermore, the morphological features of DNA concatemers were characterized by atomic force microscopy (AFM). As shown in Fig. 1C, long dsDNA copolymeric nanowires were observed for the ST-triggered HCR, while tiny dots of hairpin monomers were observed for the non-triggered HCR system. In conclusion, these results clearly demonstrate the successful assembly of DNA concatemers. Next, the MBs-DNA concatemer (MDD) complexes were formed through the streptavidin–biotin reaction. Dynamic light scattering showed that the hydrodynamic size of MBs increased from 1.0 μm to 1.2 μm (MDD) due to the conjugation of the ST-DNA concatemer layer (Fig. 1D). The zeta potential of MBs shifted to a more negative value after the conjugation of ST-DNA concatemers (Fig. 1E). UV-vis spectra show the characteristic peak at 260 nm for DNA that appeared after conjugating with ST-DNA which indicates that the DNA concatemers have already been completely connected to the surface of the MBs (Fig. 1F). These results implied the successful conjugation of the DNA concatemers to MBs.

Feasibility evaluation of the MDD-Cas12a system

The Pb^{2+} triggered cleavage of the substrate-trigger strand (ST) by the DNAzyme (DZ) was first verified (Fig. 2A) through PAGE. As shown in Fig. 2B, in the absence of Pb^{2+}, the ST strand remained intact, and no cleavage product was found in Lane 1. Meanwhile, as the concentration of Pb^{2+} increased, a corresponding increase in the quantity of the cleaved substrate was observed, progressing from lane 7 to lane 2. The detailed cleavage yield is shown in Fig. S1.† These results suggest that Pb^{2+} can trigger the release of DNA concatemers by DZ, which could efficiently trigger the trans-cleavage activity of Cas12a after magnetic separation. Then, the feasibility analysis of the MDD-Cas12a system was further conducted by monitoring the changes in fluorescence within the system. The fluorescence spectra of different sensor components are presented in Fig. 2C, and no significant fluorescence response was observed in the inactive CRISPR/Cas12a system (missing lead ions or DZ). In contrast, the CRISPR/Cas12a system was activated by the DNA concatemers released through Pb^{2+}-based DNAzyme cleavage, and an obvious fluorescence response was observed at 565 nm. The above verification indicates the feasibility of the MDD-Cas12a system for Pb^{2+} detection.

Performance of the MDD-Cas12a system

To demonstrate the quantitative detection capability of the MDD-Cas12a system for Pb^{2+}, fluorescence tests were performed under optimized conditions (Fig. S2†). As shown in Fig. 3, the MDD-Cas12a system exhibited a concentration-dependent fluorescence variation for target Pb^{2+}. A linear relationship was established between the fluorescence change and the logarithm of Pb^{2+} concentration, ranging from 0.01 to 400 nM, with a detection limit of 8.64 pM (3σ/slope). The regression equation was determined to be $546.2293 + 170.4739 \times \lg C$, with a correlation coefficient of $R^2 = 0.9964$ (Fig. 3B).

Published on 26 March 2025. Downloaded by Shanghai Normal University on 3/28/2025 7:46:19 AM.

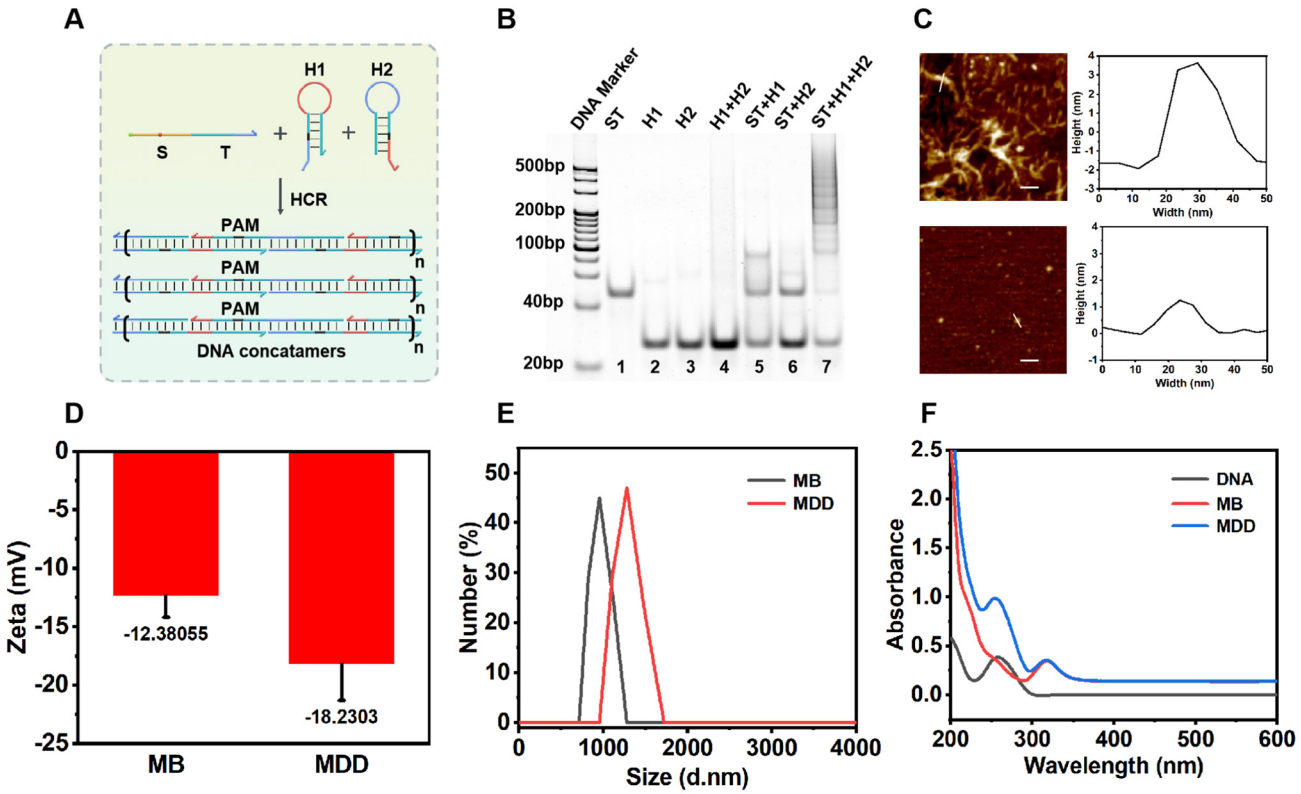


Fig. 1 Synthesis and characterization of the MDD-Cas12a system. (A) Schematic diagram of synthetic DNA concatemers. (B) PAGE characterization of the assembly of DNA concatemers. (C) AFM images of DNA concatemers. The scale bar is 50 nm. (D) Zeta potentials of MB and MDD. (E) DLS measurement of MB and MDD. (F) UV-vis spectra of MB and MDD. The data are expressed as mean ± SD (n = 3).

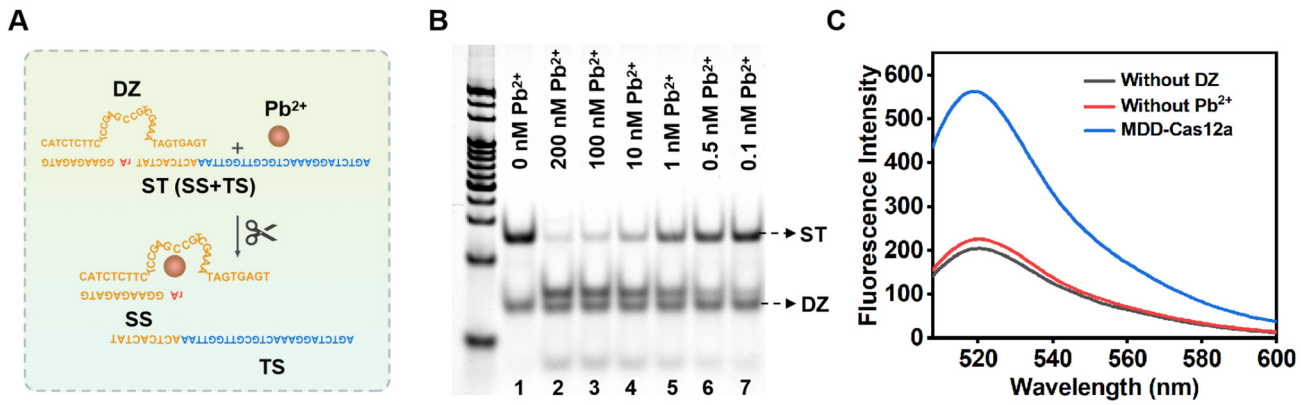


Fig. 2 Feasibility verification of the MDD-Cas12a system. (A) DNAzyme cutting diagram. (B) PAGE verifies that Pb^{2+} triggers the cutting of the substrate-trigger chain (ST) by the DNAzyme (DZ). (C) The fluorescence intensity of different sensor components.

Furthermore, stability testing of the MDD-Cas12a system for random sample analysis was conducted. In Fig. 3C–E, a total of 10 tests were performed on standard lead ion solutions with concentrations of 0.1, 1 and 10 nmol L^{-1}, and their fluorescence spectra were recorded. The results revealed relative standard deviations of 3.67%, 2.83% and 3.04% for multiple measurements at different concentrations in the standard test solutions, indicating high stability of the detection platform for random sample analysis and its suitability for quantitative lead ion analysis. Additionally, we compared the sensitivity of our system with previously reported lead ion sensors in Table S1.† The results indicate that the sensing system proposed in this study offers comparable or even higher sensitivity than most other reported sensors. The selectivity of the MDD-Cas12a system towards Pb^{2+} against other metal ions was explored by detecting 10 times higher concentrations of

 This journal is © The Royal Society of Chemistry 2025

Published on 26 March 2025. Downloaded by Shanghai Normal University on 3/28/2025 7:46:19 AM.

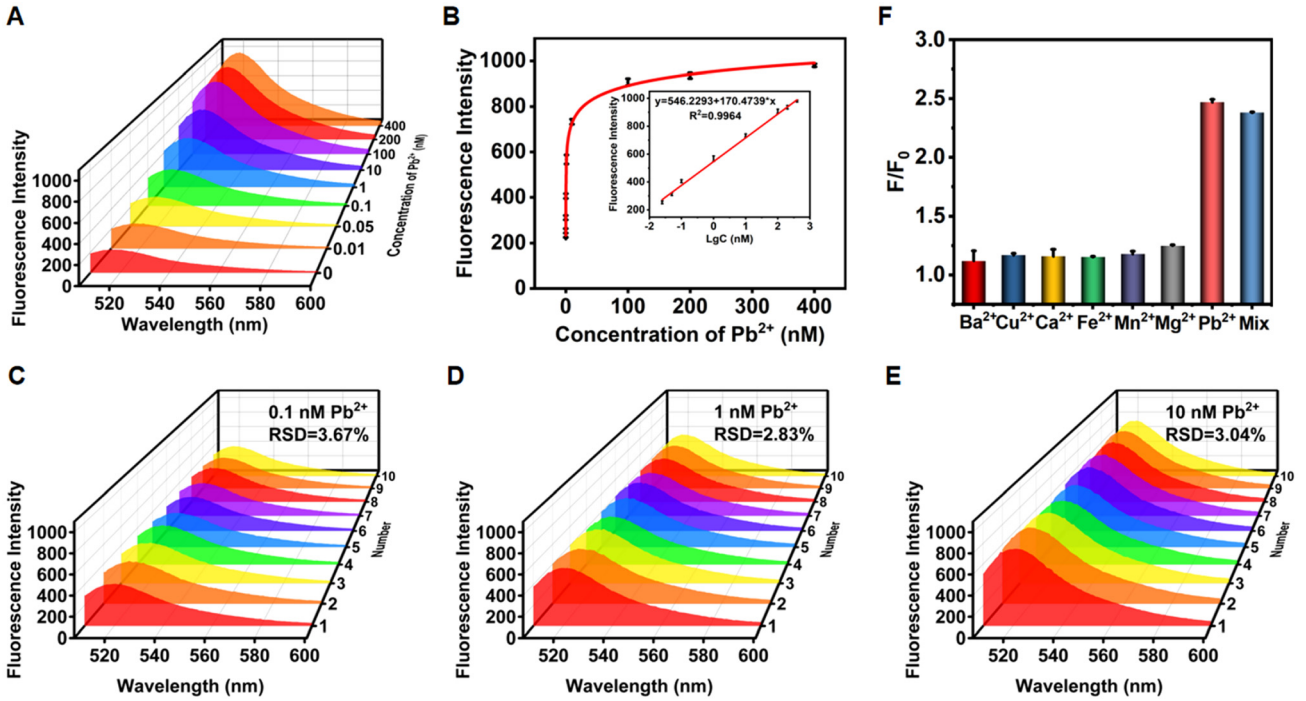


Fig. 3 Performance of the MDD-Cas12a system. (A) The fluorescence intensity of the sensor at a series of concentrations of Pb^{2+}: 0 nM, 0.01 nM, 0.05 nM, 0.1 nM, 1 nM, 10 nM, 100 nM, 200 nM, and 400 nM. (B) Linear analysis of MDD-Cas12a at different concentrations of Pb^{2+}. Data are expressed as mean ± standard deviation (n = 3). Ten stability tests were performed for Pb^{2+} solutions at (C) 0.1 nM, (D) 1 nM and (E) 10 nM. (F) Specificity of MDD-Cas12a for Pb^{2+} detection.

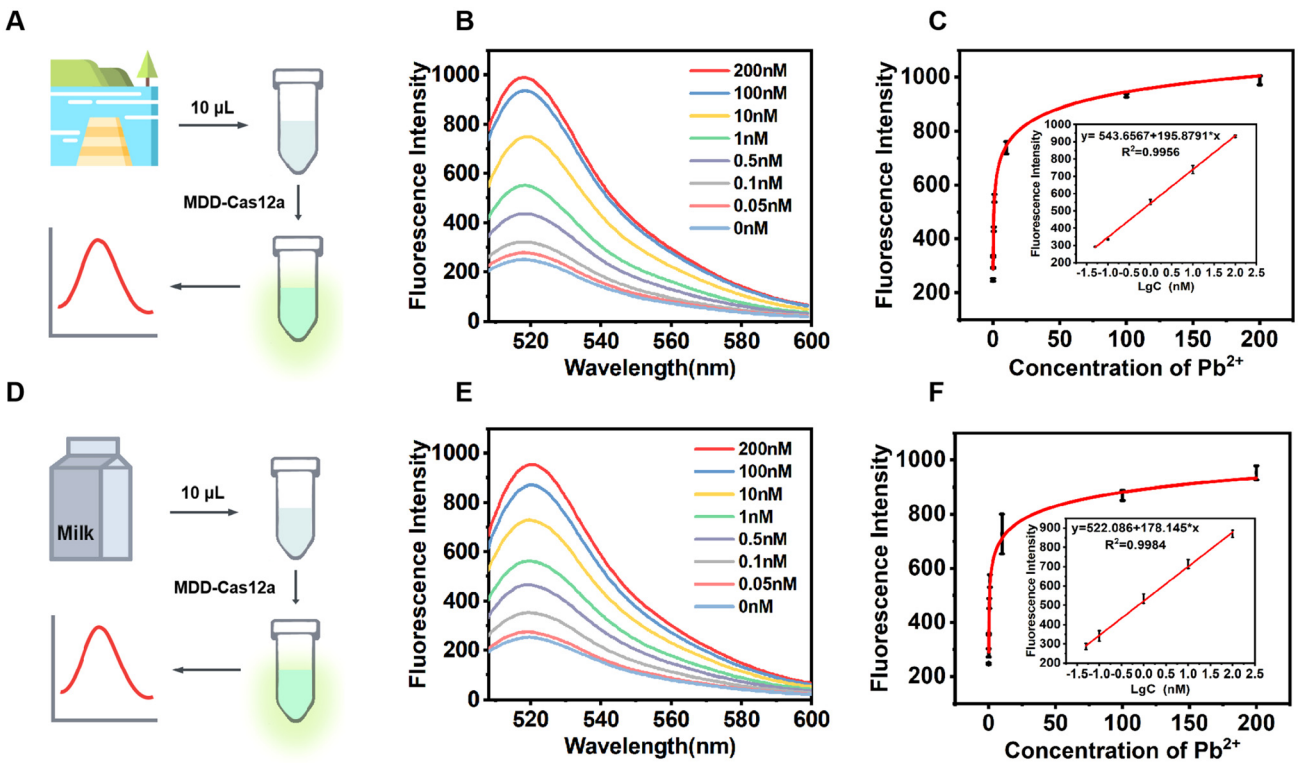


Fig. 4 Application in real samples. (A) Schematic diagram of lake water samples. (B) The fluorescence intensity of the sensor for various concentrations of Pb^{2+} in lake water. (C) Linear analysis of MDD-Cas12a at different concentrations of Pb^{2+} in lake water. (D) Schematic diagram of milk samples. (E) The fluorescence intensity of the sensor for a series of concentrations of Pb^{2+} in milk. (F) Linear analysis of MDD-Cas12a at different concentrations of Pb^{2+} in milk.

Published on 26 March 2025. Downloaded by Shanghai Normal University on 3/28/2025 7:46:19 AM.

Table 1 Comparison of Pb^{2+} concentrations in lake water and milk using the MDD-Cas12a system and ICP-MS

Samples	Added (nM)	Detected (nM)	RSD (%)	Recovery (%)	ICP-MS detected (nM)
Lake water	0	—	—	—	—
	0.05	0.0521	0.7	89	0.0839
	1	1.0921	2.6	109.2	1.0464
	10	9.9106	3.1	99.1	10.5484
Milk	0	—	—	—	—
	0.05	0.0478	5.4	95.6	0.0629
	1	1.1605	4.6	116.1	1.1918
	10	11.83	3.2	118.3	9.9139

Ba^{2+}, Cu^{2+}, Ca^{2+}, Fe^{2+}, Mn^{2+}, and Mg^{2+} under identical conditions. The experimental results showed that the MDD-Cas12a system exhibited low fluorescence signals for all interfering metal ions, and high fluorescence signals were obtained only in the presence of Pb^{2+} or Pb^{2+} coexisting with other interfering metal ions (Fig. 3F and S3†). Overall, this novel MDD-Cas12a detection platform demonstrated high selectivity and specificity for the detection of target Pb^{2+}.

Application in real samples

The large amount of Pb^{2+} in water sources will cause water pollution and affect the ecology of water, and Pb^{2+} in food will be enriched through the food chain, and ultimately affect human health. Two types of real samples, lake water and milk, were selected as model matrices to assess the applicability of the MDD-Cas12a sensor. Different concentrations of Pb^{2+} were spiked into the real samples through the standard addition method for analysis. As shown in Fig. 4, fluorescence intensities increase with increasing Pb^{2+} concentrations from 0 to 200 nM in both lake water and milk samples. The linear detection range of the MDD-Cas12a sensor for Pb^{2+} in both lake water and milk is from 0.05 nM to 100 nM. Moreover, as shown in Table 1, the recoveries of Pb^{2+} in different samples were observed in a range from 89% to 118.3%, with the highest RSD of 5.40%. Furthermore, the accuracy of our method was closely aligned with ICP-MS. Therefore, the results demonstrated that the MDD-Cas12a system is accurate and sensitive enough to detect the contamination of Pb^{2+} in the environment and food samples.

Conclusions

In summary, an innovative MDD-Cas12a system, consisting of a Pb^{2+} DNAzyme, DNA concatemer modified magnetic beads and the CRISPR/Cas12a amplification system, was designed for highly specific fluorescence detection of Pb^{2+}. The long DNA concatemers containing multiple PAM and protospacer sequences were synthesized using the substrate strand initiated hybridization chain reaction. In the presence of Pb^{2+}, the DNAzyme structure catalyzes the cleavage of the substrate strand, leading to the release of the DNA concatemers. After magnetic separation, the released DNA concatemers could activate the trans-cleaving activity of the Cas12a/crRNA complex and nonspecifically cleave the fluorescent reporter, thus enabling the quantitative detection of Pb^{2+} in the sample. Benefitting from the specific Pb^{2+} recognition ability of the DNAzyme, the programmability of the DNA concatemers, and the self-amplification ability of the CRISPR/Cas12a system, the MDD-Cas12a system exhibits extremely high specificity towards Pb^{2+} against other co-existing species and an impressive detection limit of 8.64 pM with a wide dynamic linear range from 0.01 to 400 nM. Furthermore, the MDD-Cas12a system also shows excellent detection effects in lake water and milk samples. Although the target in this assay is Pb^{2+}, the method can specifically recognize other small molecules or ions by changing the sequence of the DNAzyme in the MDD-Cas12a system, thus broadening the field of application with potential prospects.

Author contributions

Shaoying He: methodology, data curation, and writing the original draft. Wei Lin: methodology, validation and data curation, Xin Liu: methodology and investigation. Fei Li: sample collection. Hong Liang: modified the language. Huo Xu: reviewing and editing the manuscript. Chunhua Lu: methodology, reviewing and editing the manuscript. Chao Xing: conceptualization, supervision, writing – review & editing, manuscript checking and proofreading.

Data availability

The data supporting this article have been included as part of the ESI.†

Conflicts of interest

There are no conflicts to declare.

Acknowledgements

This work was financially supported by the Natural Science Foundation of Fujian (No. 2024J011177) and Research Project of Fashu Foundation (No. MFK24030).

References

1 H. Wang, L. Yang, S. Chu, B. Liu, Q. Zhang, L. Zou, S. Yu and C. Jiang, *Anal. Chem.*, 2019, **91**, 9292–9299.
2 N. Zhang, K. Shen, X. Yang, Z. Li, T. Zhou, Y. Zhang, Q. Sheng and J. Zheng, *Food Chem.*, 2018, **264**, 462–470.
3 T. Fan, Y. Liu, B. Feng, G. Zeng, C. Yang, M. Zhou, H. Zhou, Z. Tan and X. Wang, *J. Hazard. Mater.*, 2008, **160**, 655–661.

 This journal is © The Royal Society of Chemistry 2025

Published on 26 March 2025. Downloaded by Shanghai Normal University on 3/28/2025 7:46:19 AM.

4 M. W. Wensing, B. W. Smith and J. D. Winefordner, *Anal. Chem.*, 1994, **66**, 531–535.
5 K. Huang, Y. Chen, F. Zhou, X. Zhao, J. Liu, S. Mei, Y. Zhou and T. Jing, *J. Hazard. Mater.*, 2017, **333**, 137–143.
6 M. Wang, W. Feng, J. Shi, F. Zhang, B. Wang, M. Zhu, B. Li, Y. Zhao and Z. Chai, *Talanta*, 2007, **71**, 2034–2039.
7 R. Liang, J. Dong, J. Li, H. Jin, M. Wei, T. Bai, W. Ren, Y. Xu, B. He and Z. Suo, *Food Chem.*, 2024, **435**, 137503.
8 D. Morrison, M. Rothenbroker and Y. F. Li, *Small Methods*, 2018, **2**, 1700319.
9 M. J. Kellner, J. G. Koob, J. S. Gootenberg, O. O. Abudayyeh and F. Zhang, *Nat. Protoc.*, 2019, **14**, 2986–3012.
10 J. S. Gootenberg, O. O. Abudayyeh, M. J. Kellner, J. Joung, J. J. Collins and F. Zhang, *Science*, 2018, **360**, 439–444.
11 T. Tian, B. Shu, Y. Jiang, M. Ye, L. Liu, Z. Guo, Z. Han, Z. Wang and X. Zhou, *ACS Nano*, 2021, **15**, 1167–1178.
12 Y. Tang, L. Gao, W. Feng, C. Guo, Q. Yang, F. Li and X. C. Le, *Chem. Soc. Rev.*, 2021, **50**, 11844–11869.
13 M. Chen, R. Luo, S. Li, H. Li, Y. Qin, D. Zhou, H. Liu, X. Gong and J. Chang, *Anal. Chem.*, 2020, **92**, 13336–13342.
14 H. Gong, X. Hu, R. Zeng, Y. Li, J. Xu, M. Li and D. Tang, *Sens. Actuators, B*, 2022, **369**, 132307.
15 S. Gong, X. Wang, P. Zhou, W. Pan, N. Li and B. Tang, *Anal. Chem.*, 2022, **94**, 15839–15846.
16 M. Liang, Z. Li, W. Wang, J. Liu, L. Liu, G. Zhu, L. Karthik, M. Wang, K.-F. Wang, Z. Wang, J. Yu, Y. Shuai, J. Yu, L. Zhang, Z. Yang, C. Li, Q. Zhang, T. Shi, L. Zhou, F. Xie, H. Dai, X. Liu, J. Zhang, G. Liu, Y. Zhuo, B. Zhang, C. Liu, S. Li, X. Xia, Y. Tong, Y. Liu, G. Alterovitz, G.-Y. Tan and L.-X. Zhang, *Nat. Commun.*, 2019, **10**, 3672.
17 Z. Lv, Q. Wang and M. Yang, *Anal. Chem.*, 2021, **93**, 12921–12929.
18 J. Moon, H.-J. Kwon, D. Yong, I.-C. Lee, H. Kim, H. Kang, E.-K. Lim, K.-S. Lee, J. Jung, H. G. Park and T. Kang, *ACS Sens.*, 2020, **5**, 4017–4026.
19 X. Mu, J. Li, S. Xiao, J. Xu, Y. Huang, S. Zhao and J. Tian, *Sens. Actuators, B*, 2023, **375**, 132870.
20 B. Wang, R. Wang, D. Wang, J. Wu, J. Li, J. Wang, H. Liu and Y. Wang, *Anal. Chem.*, 2019, **91**, 12156–12161.
21 J. Li, S. Yang, C. Zuo, L. Dai, Y. Guo and G. Xie, *ACS Sens.*, 2020, **5**, 970–977.
22 Y. Xiong, J. Zhang, Z. Yang, Q. Mou, Y. Ma, Y. Xiong and Y. Lu, *J. Am. Chem. Soc.*, 2020, **142**, 207–213.
23 J. S. Chen, E. Ma, L. B. Harrington, M. Da Costa, X. Tian, J. M. Palefsky and J. A. Doudna, *Science*, 2018, **360**, 436–439.
24 D. Samanta, S. B. Ebrahimi, N. Ramani and C. A. Mirkin, *J. Am. Chem. Soc.*, 2022, **144**, 16310–16315.
25 Y. Chen, H. Wu, S. Qian, X. Yu, H. Chen and J. Wu, *Anal. Chim. Acta*, 2022, **1192**, 339356.
26 C. M. Green, J. Spangler, K. Susumu, D. A. Stenger, I. L. Medintz and S. A. Díaz, *ACS Nano*, 2022, **16**, 20693–20704.
27 M. Lin, H. Yue, T. Tian, E. Xiong, D. Zhu, Y. Jiang and X. Zhou, *Anal. Chem.*, 2022, **94**, 8277–8284.
28 J. You, H. Park, H. Lee, K. Jang, J. Park and S. Na, *Biosens. Bioelectron.*, 2023, **224**, 115078.
29 C. Qian, R. Wang, H. Wu, F. Zhang, J. Wu and L. Wang, *Anal. Chem.*, 2019, **91**, 11362–11366.
30 X. Fu, Y. Shi, F. Peng, M. Zhou, Y. Yin, Y. Tan, M. Chen, X. Yin, G. Ke and X.-B. Zhang, *Anal. Chem.*, 2021, **93**, 4967–4974.
31 G. Wang, W. Tian, X. Liu, W. Ren and C. Liu, *Anal. Chem.*, 2020, **92**, 6702–6708.
32 K. Zhang, Z. Fan, B. Yao, Y. Ding, J. Zhao, M. Xie and J. Pan, *Biosens. Bioelectron.*, 2021, **178**, 113019.
33 Y. Dong, C. Yao, Y. Zhu, L. Yang, D. Luo and D. Yang, *Chem. Rev.*, 2020, **120**, 9420–9481.
34 C. Y. Weng, X. Y. Li, Q. Y. Lu, W. Yang, J. Wang, X. Q. Yan, B. Z. Li, M. Sakran, J. L. Hong, W. Y. Zhu and X. M. Zhou, *Microchim. Acta*, 2020, **187**, 575.
35 C. Zhao, L. Zhang, Q. Wang, L. Zhang, P. Zhu, J. Yu and Y. Zhang, *ACS Appl. Mater. Interfaces*, 2021, **13**, 20397–20404.